

Cite this: *Lab Chip*, 2012, 12, 1917–1931

www.rsc.org/loc

Lab-in-a-tube: ultracompact components for on-chip capture and detection of individual micro-/nanoorganisms†‡Elliot J. Smith,^{§*} Wang Xi,^a Denys Makarov,^a Ingolf Mönch,^a Stefan Harazim,^a Vladimir A. Bolaños Quiñones,^a Christine K. Schmidt,^b Yongfeng Mei,[¶] Samuel Sanchez^a and Oliver G. Schmidt^{*ac}

Received 29th November 2011, Accepted 1st March 2012

DOI: 10.1039/c2lc21175k

A review of present and future on-chip rolled-up devices, which can be used to develop lab-in-a-tube total analysis systems, is presented. Lab-in-a-tube is the integration of numerous rolled-up components into a single device constituting a microsystem of hundreds/thousands of independent units on a chip, each individually capable of sorting, detecting and analyzing singular organisms. Such a system allows for a scale-down of biosensing systems, while at the same time increasing the data collection through a large, smart array of individual biosensors. A close look at these ultracompact components which have been developed over the past decade is given. Methods for the capture of biomaterial are laid out and progress of cell culturing in three-dimensional scaffolding is detailed. Rolled-up optical sensors based on photoluminescence, optomechanics, optofluidics and metamaterials are presented. Magnetic sensors are introduced as well as electrical components including heating, energy storage and resistor devices.

^aInstitute for Integrative Nanosciences, IFW Dresden, Helmholtzstr. 20, 01069 Dresden, Germany. E-mail: elliotjwsmith@gmail.com; o.schmidt@ifw-dresden.de; Fax: +49 (351) 4659-782; Tel: +49 (351) 4659-810

^bThe Gurdon Institute, University of Cambridge, Tennis Court Road, Cambridge CB2 1QN, UK

^cMaterial Systems for Nanoelectronics, Chemnitz University of Technology, Reichenhainer Str. 70, 09107 Chemnitz, Germany

† Published as part of a themed issue in collaboration with the III International Workshop on Analytical Miniaturization and NANOTEchnologies, Barcelona, 2012

‡ Electronic supplementary information (ESI) available. See DOI: 10.1039/c2lc21175k

§ Current address: GlobalFoundries Inc., Wilschdorfer Landstrasse 101, 01109 Dresden, Germany.

¶ Current address: Department of Materials Science, Fudan University, Handen Rd. 220, 200433, Shanghai, China.



Elliot J. Smith

Elliot J. Smith received his BA (2006) and MS (2007) in physics from the University of Colorado at Boulder, CO, USA, and was the recipient of the Physics Tradesman Award (2006). He received his PhD (2011) in experimental physics from the Chemnitz University of Technology, Germany. The work was carried out at the IFW Dresden, for which he received the Tschirnhaus-Plakette for best PhD 2011. He was a group leader at the IFW Dresden before taking his current position in the semi-

conductor industry as a Sr. Process Engineer at GlobalFoundries. His research interests include physics, optics, metamaterials, on-chip integration, semiconductors and nanotechnology.



Wang Xi

Wang Xi received his BS in chemistry from the University of Science and Technology of China in 2004. As a Dorothy Hodgkin Postgraduate Award winner in 2004, he went to the University of Oxford for a PhD in chemistry, which he received in 2009. He was a post-doctoral researcher in the Department of Biochemistry, University of Oxford, under the supervision of Professor Anthony Watt from 2009 to 2010. He joined the IFW Dresden as a post-doctoral researcher in 2010.

His current research interests are single cell behavior inside highly defined 3D rolled-up microtubes and intelligent micro/nano-engines for biosensing.

1 Introduction

The concept of lab-on-a-chip aims to bring the functionality found in a laboratory down to a chip which can fit in the palm of a hand.^{1–8} This total analysis system scale-down can lead to many advantages, one of which includes the ability to have on-the-go, in-the-field diagnostics. Another benefit is that as smaller and more sensitive detectors and devices are developed, reduced amounts/quantities of fluids/specimens are required for a full analysis. In fact, the demonstration of efficiently analyzing and manipulating molecular reactions on micro-/nanometre scales has been shown.⁹ Decreased analysis intervals and increased rates of response are also possible due to the reduced flow distances and faster heating speeds of these compact systems—not to mention the minimal fabrication costs. One of the big challenges in designing lab-on-a-chip microanalytical devices involves the integration of microfluidics and suitable micro-

nanotechnologies which can bring new and compact functionalities to the system.

Microfluidic systems should combine a series of components such as small-scale methods to introduce the samples into the microchannels, pumping the fluids throughout the chip, and detection systems that can allow for sensing and read-out of those results. Therefore, a requirement of lab-on-a-chip systems is that the system be capable of a large-scale integration of numerous components. A dream in nanotechnology and analytic systems is to fabricate a device which integrates several of these functionalities into a single chip which would lead to improved performance and compactness, be user-friendly and combine different detection methods. With regards to introducing a sample into the device, several approaches have been proposed such as electrokinetic forces inducing electroosmotic flows. This could be achieved with the integration of electrodes into the chip, as opposed to the alternative pressure-driven flow commonly



Denys Makarov

Denys Makarov obtained his Masters Degree (2005) at the Taras Shevchenko National University of Kyiv in Ukraine, followed by a PhD (2008) from the University of Konstanz in Germany. His research interest is in fundamental and applied aspects of modern magnetism, in particular magnetization reversal and coupling phenomena in magnetic thin films and heterostructures on curved surfaces and the development of shapeable (flexible and stretchable) magnetic sensors. Since 2010, Denys

Makarov is leading the group “Magnetic Nanomembranes” (MAGNA) at the Institute for Integrative Nanosciences, IFW Dresden, Germany.



Yongfeng Mei

Yongfeng Mei received his PhD at City University of Hong Kong in 2005. After that, he joined the Max Planck Institute for Solid State Research as a post-doctoral researcher. In 2007, he moved to IFW Dresden as a group leader in the Institute for Integrative Nanosciences. In 2010, he joined the Department of Materials Science, Fudan University, China, as a full professor in materials chemistry and physics. His research interest focuses on the development of novel inorganic nanomembranes.



Samuel Sanchez

Samuel Sanchez received his PhD at the Autonomous University of Barcelona, Spain, in 2008. He studied and developed new composite materials for the construction of electrochemical biosensors based on soft polymers, carbon nanotubes, and metallic nanoparticles. After one year as assistant professor at the Autonomous University of Barcelona, he joined the ICYS at the International Research Center for Materials Nanoarchitectonics, National Institute for Materials Science, Japan, in February 2009 on a tenure track. In May 2010 he

joined the Institute for Integrative Nanoscience at the IFW Dresden where currently he is leading a group working on nanobiochemical applications of nanomembranes.



Oliver G. Schmidt

Oliver G. Schmidt is a Director at the IFW Dresden, Germany, and holds a full Professorship for Material Systems for Nanoelectronics at the Chemnitz University of Technology, Germany. His scientific activities are based on quantum dots and nanomembranes, bridging across interdisciplinary research fields: from nanophotonics via on-chip energy storage to nanorobotics and microbiology. He has received several awards: the Otto-Hahn Medal from the Max-Planck-Society in 2000, the Philip-Morris Research Award in 2002 and the Carus-Medal from the

German Academy of Natural Scientists Leopoldina in 2005. Most recently in 2010, he was awarded the Guinness World Record® for the smallest man-made jet engine.

produced by external valves and pumps. By replacing these external system dependencies, a further shrink-down of the device is possible. Developing microchannels with a tunable size, on demand, is also of interest for broadening the applications of such a device as well. For instance, if molecules (requiring small channels) or cells (requiring larger channels) need to be detected, a versatile platform for designing on-demand scaled microchannels is important.

The detection techniques used in microfluidics have been extensively investigated as well. Highly sensitive methods are needed because the small sample volume which is confined to the microchannels generally leads to smaller detectable signals. A common classification could be separated into optical and electrochemical detections, although numerous other techniques have been also explored. Among the possibilities for electrochemical detection, the combination of nanomaterials such as carbon nanotubes (CNTs) or nanoparticles with microanalytical methods has been successful in the detection of food samples,^{7,10} pharmaceutical samples,¹¹ explosives,¹² and pesticides,¹³ whereas optical detectors have shown to be useful in a wide variety of other applications. Examples can be found for the detection of water pollution¹⁴ and even in pregnancy tests, which are based on the plasmonic sensing¹⁵ of an antigen–antibody reaction.¹⁶

In the spirit of developing increased functionality in more compact lab-on-a-chip systems, lab-in-a-tube goes further and aims at condensing an entire laboratory into an even smaller, micron-scaled package. This system is the next scale-down in smart lab-on-a-chip cellular platforms and would have all the functional and sensing components necessary for stimulating and analyzing individual organisms comprised in a single microtube. In addition, such a system could be used to collect data in a highly parallel fashion given the ability to create large arrays of tube devices on a single chip. Lab-in-a-tube would therefore address the importance of understanding organisms at an individual level while, at the same time, meeting the standards of biological studies which require a high amount of statistics for data analysis.

The backbone of the lab-in-a-tube system are microtubular architectures, which are fabricated through a nanotechnology based self-assembly process. By using strain engineering¹⁷ methods, researchers have been able to expand a classical two-dimensional (2D) system into the third dimension through the release and roll-up of pre-strained nanomembranes.^{18–24} The result is the creation of large arrays of on-chip microtube structures. Rolled-up nanotech has allowed for the development of many on-chip integrated devices, such as optical modules,^{25–35} chemical pumping systems,³⁶ and electrical components^{37,38} (including ultracompact energy storage devices^{39–41} and superconductors⁴²), as well as provided three-dimensional (3D) scaffolding for cell culture experiments.^{43–47} This review will serve to provide an examination of many of these individual rolled-up devices. Furthermore, through the combination and integration of these single components, researchers will be able to fully develop the system known as lab-in-a-tube.^{28,48,49}

Each lab-in-a-tube ideally integrates a number of functional rolled-up ultracompact components into a single device, Fig. 1. The final version of such a device could have an integrated pumping system for capturing and extracting biomatter for testing. There would be electrodes integrated within for data

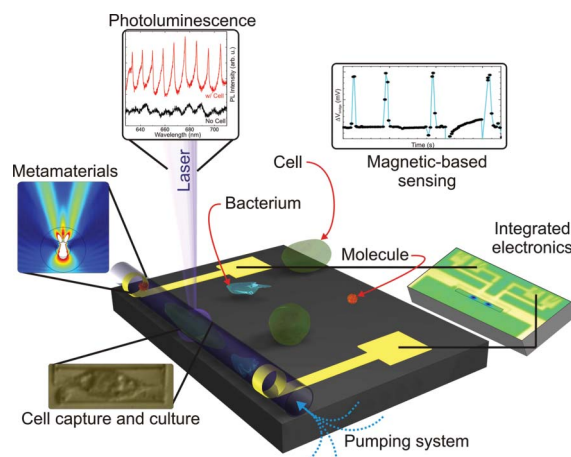


Fig. 1 A lab-in-a-tube device comprises numerous ultracompact components in a single tube which can be developed using rolled-up technology. A single device, being one of thousands in the on-chip system, would be independently capable of stimulating, monitoring and investigating individual organisms.

collection, including resistive measurements³⁷ and energy storage devices.^{39–41} Numerous optical sensors based on optical ring resonators^{25,27,34,35,50,51} and metamaterials^{29,31,32,52} can be implemented as well. Cell culturing can be influenced through a functionalization⁵³ of the inner wall of these microtubes, for instance to mimic the extracellular matrix (ECM), providing a comfortable platform for the cells to grow. Built-in heating devices⁵⁴ can be employed to locally investigate cellular response to incubation. Magnetic sensors relying on the giant magnetoresistance (GMR) effect can also be integrated.⁵⁵ Much progress, as will be presented below, has been made in the design and implementation of all of the mentioned ultracompact components.

2 Capturing of biomaterials

For lab-in-a-tube systems to function efficiently, methods for capturing organisms into the tubular structure must be developed. Ideally, such a capturing system would be developed as another integrated component, which would rely, for instance, on electroosmotic flow,⁵⁶ controllable with electrodes, or some other chemical pumping system.^{36,57,58} Other possible solutions, which have been developed previously, rely on an external system for the manipulation of biomaterial, in particular, cells. One such system is known as a microsyringe pump.²⁸ In this section an overview of the capturing systems, thus far developed for lab-in-a-tube, will be presented.

2.1 Microsyringe pumping system

A microsyringe pumping system is a pump which acts as a microvacuum used to suck up a cell-rich culture medium.²⁸ A microfluidic pump is connected to a replaceable nozzle *via* plastic tubing. The nozzle is mounted onto an XYZ micromanipulator for fine-tuned spatial manipulation of the vacuum. The nozzle is made up of a glass capillary which has been tapered down to a diameter on the scale of tens of micrometres (usually ~ 14 to $50 \mu\text{m}$). This nozzle is positioned with the micromanipulator to one end of an on-chip microtube, Fig. 2(a) and (b). Once the

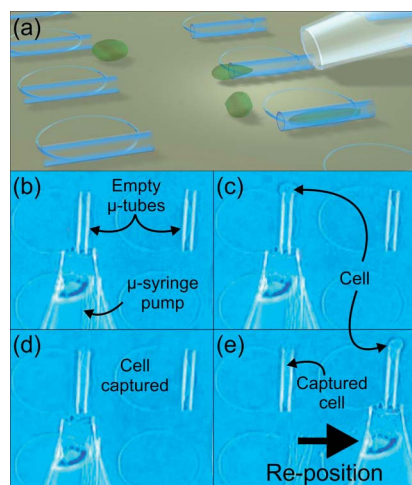


Fig. 2 Microsyringe cell pumper.²⁸ (a) Using a tapered capillary as the nozzle of a microfluidic pump, an efficient method for capturing cells is created. (b) The nozzle is placed at one end of a microtube. (c) After the pump is turned on, a cell is captured at the other end of the microtube and due to the sucking force, the cell is brought within the confinement of the tube (d). (e) The nozzle is then positioned to another microtube and the process is repeated. Adapted from E. J. Smith *et al.* (ref. 28).

microfluidic pump is switched on, the cell-rich medium is sucked through the microtube at a pump rate of $0.01\text{--}0.1\ \mu\text{L s}^{-1}$, and, eventually, a cell is drawn to the end of the microtube (opposite from that of the microsyringe), Fig. 2(c). Even if much larger than the microtube, the cell can be forced/pulled into the confinement of the tube, Fig. 2(d), by applying an increased pump rate (pump rate of $0.5\text{--}1\ \mu\text{L s}^{-1}$). After a cell is fully inside, the pump is turned off and the nozzle can be easily positioned to the opening of another microtube in the array, after which the process is repeated, Fig. 2(e).

The technique is cheap and easy to use and therefore well-suited for operation in research laboratories. Another feature of this method is the ability to “force” oversized cells into the confinements of the tubes because of the high achievable suction force of the system. Disadvantages of the method include a high loss of cells from the sample (many are sucked into the microsyringe and lost) which could be a problem if the cell concentration is low. This also means that a particular cell cannot be easily singled out for capture. Another aspect which requires further study is the physical impact the suction exerts on the cell, and whether or not a cell is damaged, and if so, up to what extent.

2.2 Optical trap system for cell manipulation

Another off-chip system for cell manipulation relies on the trapping power of light to capture cells near the surface of the substrate and manipulate them into the microtubes. This technique, called optical trapping,⁵⁹ is used to capture cells at the beam waist of a laser which is focused down onto the cell with a high magnification objective, Fig. 3(a). Optical trapping systems have not only been used for interesting biomatter manipulation⁶⁰ but also to study the microdynamics and biomechanics exhibited by cells and bacteria.^{61–63} The trapping is achievable because of the radiation pressure exerted on the

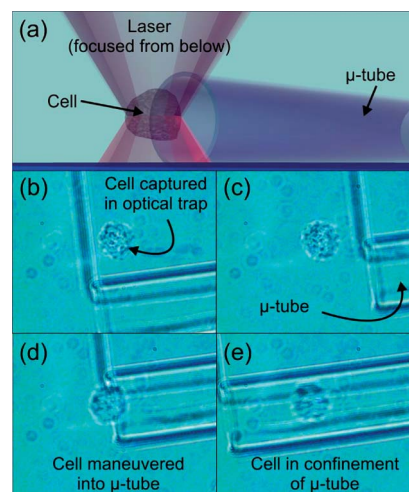


Fig. 3 Optical trap for capturing cells. (a) Using the confining force offered by an optical trap system, cells can be singled out and (b) captured, (c) maneuvered over to the (d) opening of a microtube and brought within the confinement of the microtube (e).

cell/microobject by the laser. This is possible for a cell which has a higher index of refraction than the surrounding media. Forces act on the microobject due to Fresnel reflection and refraction at the surface of the object from the incoming and outgoing beams.⁵⁹ These forces can either lead to an acceleration (shooting) of the microobject [particularly likely if the index of refraction is much higher than the surroundings, or highly reflecting (metallic)] or, as is the case presented here, the exerted forces trap the microobject at the beam waist. In other words, whether or not the object is trapped or shot away is determined by the reflection and deflection forces.

Using an optical trap with a laser diode of wavelength $\lambda_0 = 975 \pm 1\ \text{nm}$ [tunable power ($0\text{--}330\ \text{mW}$ at output of laser)], whose light is focused down with a $100\times$ objective, we have been able to manipulate individual cells on-chip, Fig. 3(b) and (c). This manipulation has allowed us to capture cells which reside freely in the culture medium and bring them into the confinement of our microtubes, Fig. 3(d) and (e). This has proven to be an excellent approach for capturing a particular cell of interest. Preliminary results suggest that the cells are not destroyed by the laser light, and will continue to proliferate after the manipulation. However, more experiments still need to be performed to investigate the survival rate of cells which have been manipulated in such a manner. The downsides of this method are that, although a particular cell can be singled out and manipulated on-chip (an advantage over the previously mentioned approach), the forces exerted on the cell by the trap are not strong enough to pull an oversized cell into a microtube. This means that when using this technique, the microtubes must be larger than the cell of interest.

2.3 Catalytic pumping system

The pumping of fluid at the microscale is challenging due to the high viscosity dominating at low Reynolds numbers.⁶⁴ An elegant integrated on-chip approach of pumping fluid without help from external sources relies on the catalytic reactions that

can take place on the inner wall surfaces of the microfluidic pumps.⁶⁵ In particular, catalytic microtubes, containing thin Pt films in their interior, accelerate the decomposition of H_2O_2 into O_2 and H_2O , inducing a flow, and hence a pumping of fluid, through their hollow structure.³⁶ Such micropumps have the advantage of being fully autonomous and require a very low concentration of chemical fuel (hydrogen peroxide) to be activated by the generation of oxygen microbubbles. A minimum peroxide concentration of 0.06% v/v is sufficient to generate microbubbles inside the catalytic rolled-up micropumps, which is two orders of magnitude lower than reported previously.⁶⁶ In addition, at this low concentration range, an 'ON/OFF' switching of the pumps can be achieved using light, which can be provided by the observation microscope.⁶⁷ On top of this, it has been shown that the pumping rate of such microtube systems is increased when working at physiological temperatures (*i.e.* 37 °C).⁶⁸ This suggests that losses in pump performance, induced from driving down the fuel concentration, may be balanced out by working at increased temperatures. The fabrication of catalytic rolled-up micropumps offers compact fluid pumping as well as easy integration into lab-on-a-chip devices. The directed motion of polystyrene microparticles through these microtubular pumps was demonstrated and the unidirectional flow was used to move microparticles through the tubular structure in a directed fashion, Fig. 4. Since the diameter of the microtubes (T_d) can be tailored, the tubular micropumps could be used for sorting of particles with different sizes (P_d), Fig. 4(a) and (c).

We believe that the design of self-actuated micropumps will be of great interest for the directed transport and sorting of objects without the need for external sources in microanalytical devices.

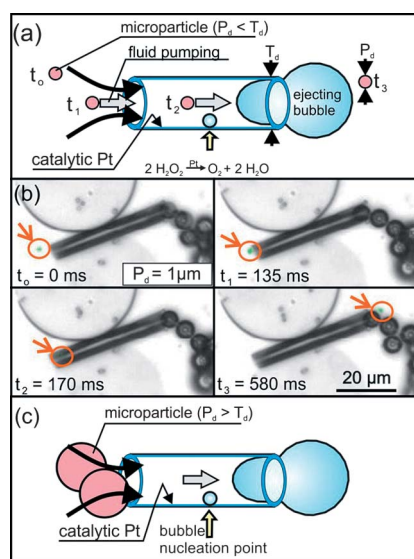


Fig. 4 On-chip chemical pumping. (a) A nanomembrane composed of platinum, making up the inner wall of a microtube, allows for the catalytic breakdown of H_2O_2 , present in a low concentration within the medium, into O_2 and H_2O . The oxygen bubbles created from the breakdown are ejected out of one end of the pump, generating a flow (b) which can be used to pump microobjects. Given that the diameter of the microtube limits the size of the pumpable microobjects (c), such a system would be ideal for size-sorting of microobjects. Adapted from A. A. Solovov *et al.* (ref. 36).

In addition, the use of reduced amounts of toxic fuels to efficiently move fluids is of current interest for microfluidic applications for future biomedical sensing. Such versatile micropumps may offer many advantages for integration into lab-in-a-tube analytical systems.^{28,49} For instance, the pumping of different kinds of cells into the microcavities can be envisioned by using tunable catalytic microtubes/pumps.

The toxicity of the pumping solution is of high importance for biological tests. For this purpose, researchers need to continue to push the limits of these chemical systems and consider moving to completely non-toxic environments. Again, another pumping system would rely on the pumping of an electrolyte through electroosmotic flow⁵⁶ which would require integrated electrodes, an advancement in rolled-up technology that has been realized and will be discussed later. Another promising pumping system which has been demonstrated relies on water splitting due to the illumination of TiO_2 thin films with ultraviolet light.⁶⁹ It is important to note that rolled-up microtubes can also be integrated into microfluidic channels and used for sensing purposes, a detail also highlighted later in this text.

3 Cell culture in tubular 3D scaffolding

Typical mammalian cells in tissues are constantly in contact with the 3D extracellular matrix. Adherent cells form filopodia, cytoplasmic projections spreading beyond the leading edge of migrating cells, in order to detect and interact with the complex ECM architecture. The filopodia are then transformed into lamellipodia that adhere to the ECM ligands *via* transmembrane integrin receptors.^{70–73} The ECM provides highly complicated, local, micro- and nanoscale chemical and topographical patterns,⁷⁴ which can regulate cell behavior *in vivo*.^{75,76} The competition between chemical and topographical cues in affecting cells has been deeply studied in literature.^{77,78} Developing well-defined architectures that mimic a 3D ECM for tissue engineering scaffolds is thus of great interest in life science, since these platforms have a better biological or clinical relevance if the confined cells exhibit 3D phenotypes in a similar fashion to the cells *in vivo*.

Besides recapitulating the multi-cellular complexity of a tissue more faithfully than a traditionally 2D flat culture, these 3D scaffold cell culture systems could offer several advances and conveniences in drug discovery,⁷⁹ generating realistic *in vitro* models of disease.⁸⁰ Furthermore, recent studies have demonstrated significant differences in cellular behaviors, such as differentiation,⁸¹ gene expression⁸² and drug metabolism⁸³ in 3D and 2D systems.

Advances in micro-/nanofabrication have enabled researchers to fabricate 3D cell culture scaffolds in various forms, such as microspheres,⁸⁴ microfiber networks,⁸⁵ and porous solids,⁸⁶ microarrays,⁸⁷ and microwells.⁸⁸ Among these 3D microarchitectures, microtubes can be considered as an *in vitro* mimicry of vessels, muscles, myelin, and bone tissues. With a good directionality, 3D microtubular structures can be conveniently used as pre-patterned scaffolds for the guidance of the outgrowth of living cells within, and in cell migration studies. As a microreactor with strict 2D confinement for living cells, the microtubes can be also used to study the mechanical interaction between cells and their environment. The mechanically induced

cell deformation would cause variance in cellular viability, function and gene expression.⁸⁹

Mass production of microtubes made from a variety of materials has been realized with rolled-up nanotech.^{21,23,90} In particular, transparent microtubes composed of glass (SiO_x) or sapphire (Al_2O_3) thin films enable a detailed study of the phenomena happening in their interior by optical and fluorescent microscopy techniques. Numerous biocompatible materials have been used in the creation of rolled-up microtubular structures and have been applied to cell culture analysis.^{43,44,46,47} Even if the material used in the rolled-up process is non-biocompatible, post-processing after roll-up can include an atomic layer deposition (ALD) of materials found to be biocompatible, covering the entire sample, and thus protecting the biomatter from the toxic material. This ALD also serves to better stabilize the microtubes and can be used to increase the index of refraction which can be advantageous for the optical ring resonator applications discussed later.

3.1 Yeast cells

Due to the strict directionality of the microtubes, one can also expect the guidance of cell growth, division, and migration along the tube length. For instance, yeast cells have been encapsulated inside rolled-up Al_2O_3 microtubes.⁴³ These single cell organisms are usually grown in suspension and are a well-established model cell for studying evolutionarily conserved processes, such as the cell cycle and chromosome biology.

Yeast cells were diffused into Al_2O_3 microtubes with a series of diameters, Fig. 5(a), and the cell growth was observed *in situ* with an optical microscope. Due to the 2D confinement, yeasts adapt different arrangements within the microtubes depending on the tube diameters. In a relatively large microtube (diameter $\sim 14 \mu\text{m}$), where the cell budding is not overly confined, yeasts can arrange into two separated rows. When the diameter of the tube is decreased down to $\sim 5.5 \mu\text{m}$, the mother cell rotates to efficiently use the space for its bud and a zigzag arrangement is formed. In a tube with a diameter similar to or even smaller than the cell diameter, the confinement becomes so restricting that the cell budding results in a straight row. These yeast cells were studied for periods of over 15 h inside the microtubular structures.

In order to perform long-term studies, more biocompatible materials/substrates are desired which could mimic the *in vivo* micro-environment. One solution is the fabrication of microtubes with fully biodegradable materials. A demonstration of this was recently made using self-rolled polymeric tubes based on patterned polysuccinimide–polycaprolactone bilayers in order to capture and study *in situ* seeding of yeasts during the formation of the scaffold.⁴⁶

3.2 Neuron cells

Rolled-up nanotech has been employed to pre-pattern microtopographic substrates to investigate their influence on the protrusion of neurites, Fig. 5(b).⁴⁴ In comparison with neurons that grew on a flat surface and formed random neurite networks, the cell extensions on microtube arrays tend to align in the direction of the microtubes and the arrangement appears complex and square-shaped. Moreover, the microtubes can act as

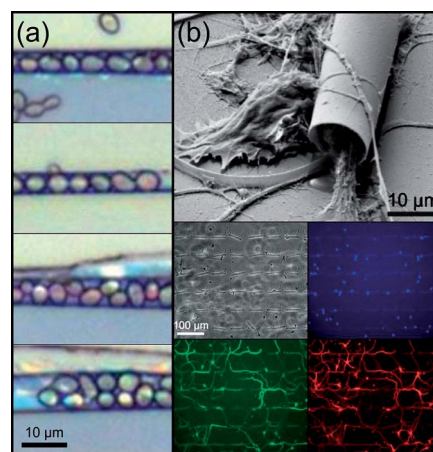


Fig. 5 Confinement of different kind of cells into microtubular structures. (a) Assembly of yeast cells inside transparent microtubes, with increasing diameters, top to bottom. The 2D-confinement of the microtubes results in the arrangement of yeast cells in a straight row in small microtubes and in a zigzag pattern in large microtubes. Adapted from G. S. Huang *et al.* (ref. 43). (b) Top: SEM image of neurons cultured with rolled-up SiO/SiO_2 microtubes. Neurons tend to grow by following the pre-patterned structure. The extending of the neurites into the microtube is clearly visible. Bottom: optical microscope images of fluorescently stained mouse neurons grown on microtubular structures show the outgrowth of the neurites along the patterned substrate, leading to the formation of square-shaped, grid-like neuronal networks. The neurons are stained with DAPI (blue) for nuclei, AlexaFluor488 (green) for axons and AlexaFluor568 (red) for the neuron outgrowth. Adapted from S. Schulze *et al.* (ref. 44).

protective coats against phototoxicity and other stress conditions from the environment acting on the neuronal cells.⁸⁹

This work on microtube-array pre-determined neurite networks was later extended to a semiconductor substrate.⁴⁵ As *in vivo* protrusions of axons are often unsheathed by glial cell membranes (myelin),^{91,92} the semiconductor Si/SiGe microtubes, where neurites outgrew from within, could thus mimic the dielectric layer wrapping around the axons. The authors claimed the integration of a “cuff electrode” where a semiconductor electric network for cell culture and physiological measurement is possible. The implementation of electrical contacts within the tubular structures will be beneficial for facilitating the electrical coupling between neurons and electrodes, and enhance the nerve stimulation while reducing the stimulus current.^{93–95}

3.3 HeLa cells

Most recently, a study which goes a step further to perform living cell studies of mammalian cells by biofunctionalizing the surface of the microtubes with proteins from the ECM has been made, Fig. 6(a).⁴⁷

The biological viability of the microtube array has been tested with single cell organisms and higher eukaryotes, such as HeLa cells, Fig. 6(b). As shown in Fig. 6(b), HeLa cells cultured on topographic substrates containing rolled-up SiO/SiO_2 microtubes show normal morphology. They survive and proliferate both inside and outside the tube for an extended period of time. This tubular structure allows only one dimension of freedom for the cells, and as a result, the cells trapped inside a microtube

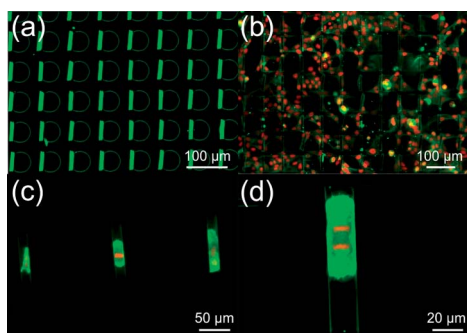


Fig. 6 Array of biocompatible microtubes with HeLa cell cultures. (a) An array of rolled-up SiO/SiO₂ microtubes biofunctionalized with fibronectin and tagged with a primary mouse antibody against fibronectin, followed by fluorescent anti-mouse IgG-FITC secondary antibody. The green fluorescence confirms the conjugation of fibronectin to the microtube surface. (b) Fluorescent image of HeLa Kyoto cells, stably expressing a fluorescently tagged core histone, H2B-mcherry (red), and mEGFP- α -tubulin (green),⁹⁶ cultured on a SiO/SiO₂ microtubes array. The cells grow well, both on the surface of the microarray and inside the microtubes, over long time periods. The green fluorescence of the tubes is due to the immunofluorescence staining as described in (a). (c) Fluorescent image of HeLa cells trapped inside microtubes. The cells are at different stages of the cell cycle: interphase (left), mitosis (middle) and two daughter cells at interphase after mitosis (right). The cells are fixed and stained with DAPI (red) for DNA and phalloidin-FITC (green) for actin. (d) A zoomed-in fluorescent image of a HeLa cell at anaphase inside a microtube. The 2D-confinement of the tubular wall prevents the cell from fully rounding-up during mitosis, but instead, forced it to take on a cylindrical shape. The cell is fluorescently stained as described in (c).

usually adapt an elongated shape, Fig. 6(c), even during mitosis when HeLa cells are normally fully rounded up. Furthermore, the cells inside the microtubes can be enriched for different stages of the cell cycle, Fig. 6(c). In contrast to bulk experiments where the data are obtained from averages of large populations, the lab-in-a-tube microsystem allows the acquisition of one dataset per cell, avoiding the loss of heterogeneities present within a population of cells. Yet, the simultaneous read-out of large amount of data from individual isolated cells within these microreactors can be obtained by simple optical fluorescent microscopy, Fig. 6(d).

These and other studies have spawned the hunt for geometrical and mechanical cues that determine cell division orientation in single cells, a step crucial for cell differentiation as well as tissue and organism development.^{97–100}

4 Optical detection components

Important detection systems, which lab-in-a-tube systems rely on, are based on optics, whether it be an optical microscope for observation or an integrated optofluidic detector. With optics, by using a number of different devices, label-free biological detection can be performed. With regards to the types of devices which can be developed using rolled-up nanotech, a number of structures have been designed to function as optical ring resonators,^{25,27} optical fibers,^{26,32} and metamaterial devices.^{29,31,32,52} Another important aspect of these 3D structures is that not only can they have optical devices built in, but the hollow tubular architectures can also act as on-chip fluidic channels.¹⁰¹ This, as will be

presented, can allow for integrated optofluidic sensors.¹⁰² The following section will outline some of these most interesting optical devices which have been investigated and planned to become an integral part of lab-in-a-tube systems.

4.1 Optical resonators for chemical sensing

As mentioned above, optical ring resonators can be created using rolled-up technology and it has been found that light can be efficiently confined to the subwavelength wall of the structures.^{25,27} The resonance is based on the constructive interference of light traveling around the circumference of the microtube, Fig. 7. When photoluminescence (PL) spectroscopy is performed, this interference pattern shows up as resonant peaks, known as whispering gallery modes (WGMs). The light source can either be embedded in the wall of the resonator, *i.e.* quantum dots²⁵ or Si nanoclusters,^{27,28,30,103} or a light source can be added into the core of the structure.¹⁰⁴ The mode number is determined by $M = n_{\text{eff}}\pi D_{\text{avg}}/\lambda_0$, where D_{avg} is the average diameter, λ_0 is the free space resonant wavelength and n_{eff} is effective index of refraction.

Given that the wall is of subwavelength thickness, a majority of the propagating evanescent field extends out of the wall. This extension can be used to probe the surrounding media and therefore n_{eff} is influenced not only by the index of refraction of the resonator material, but also by the surrounding media. Therefore, a slight change in the index of refraction of the medium translates into a slight change in n_{eff} , thereby shifting the peak position of M , allowing for a sensing of the surrounding medium, inset of Fig. 7.³⁰ Furthermore, optical resonators can also be used for label-free detection of particles or viruses^{105–107} at the surface of the wall because of an increase in the optical path length. Since rolled-up resonators assume the form of a spiral scroll, mode splitting^{108,109} can be observed (due to different optical path lengths of light travelling clockwise and counterclockwise). This is a phenomenon which can be used to detect the size^{109,110} and location of nanoparticles/nanoorganisms on the surface, as well as their distance away¹¹¹ from the surface, of the resonators. These are a number of examples

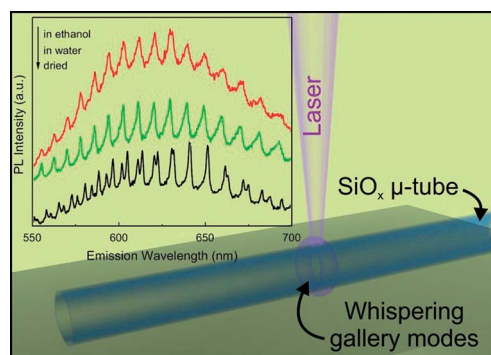


Fig. 7 Rolled-up optical ring resonator sensors. Rolled-up dielectric tubes can be used as optical ring resonators for photoluminescence experiments. The plots show the detection of changes in the surrounding media (due to different index of refraction) through slight shifts in the whispering gallery modes. Spectra adapted from G. S. Huang *et al.* (ref. 30).

showing the potential applications of optical ring resonators for biological and chemical sensing for the lab-in-a-tube family.

4.2 Flexible split-wall microtube resonator sensors (F-SW μ RS)

Another rolled-up optical resonator, which has been recently introduced and investigated for the detection of single cells, works on a slightly different sensing mechanism than those mentioned above. Rather than detecting changes in the surrounding index of refraction and particles on the surface of the resonator which lead to shifts in the WGMs, this sensor relies on an optomechanical detection of a cell's presence through an improvement over the quality factor of the resonator. The quality factor is a measure of how well light resonates around the structure and is a measure of the sharpness of the modes, defined as $Q = \lambda/\Delta\lambda$ (*i.e.* the sharper the peak in the spectrum, the higher the quality factor). The sensor discussed here is called a flexible split-wall microtube resonator sensor (F-SW μ RS),²⁸ and earns its name from an engineered nanogap which resides in the wall of the resonator. This nanogap, which is present between consecutive windings of the nanomembrane, is flexible and is forced closed when an oversized cell is brought within the confinement of the microtube.

Photoluminescence measurements are first performed on an F-SW μ RS containing no cell, top Fig. 8(a). A cell can then be sucked into the microtube using the method described by Fig. 2 (here an embryonic mouse fibroblast). After the cell is forced into the microtube, the PL measurement is repeated, revealing an increase in the quality factor of $\sim 20\times$, bottom Fig. 8(a). This is explained schematically in Fig. 8(b). Because the cell is intrinsically larger than the microtube, once it is inside the microtube, it exerts an outward force on the tube wall, thereby closing the nanogap. The effect the closing of the nanogap has on the light confinement is modeled by finite-difference time-domain (FDTD) simulations, Fig. 8(c). It is evident from the intensity profile, that the light confinement is higher once the nanogap is closed. This is due to less light being scattered by the nanogap out of the microtube. This therefore demonstrates that mechanical interactions of a living cell with the microtube structure can be detected optically.

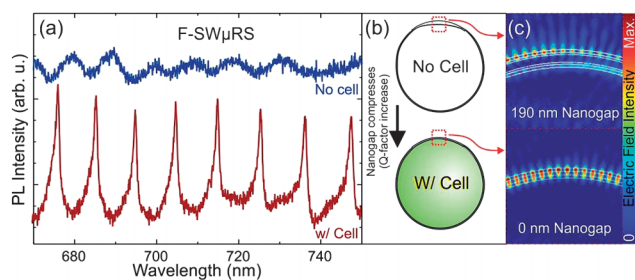


Fig. 8 Flexible split-wall microtube resonator sensors.²⁸ A method for the optomechanical detection of cells in microtubes. (a) The PL spectrum from a microresonator before and after the capture of a cell. (b) The sensing mechanism lies in the mechanical closing of a nanogap, present in the wall of the resonator, when a cell pushes outwards from inside the microtube. (c) Finite-difference time-domain simulations confirm the higher confinement of light when the flexible nanogap is closed, seen in the intensity profile of the cross section of the resonator. Adapted from E. J. Smith *et al.* (ref. 28).

This type of detector was found to be reproducible, shown by a number of independent experiments. It was also shown that a single F-SW μ RS could be used to measure consecutively captured cells. Once a cell is evacuated from the sensor, the nanogap slightly reopens, but there remains a memory of the previous cell. This could be used as a method for determining which lab-in-a-tube devices should be focused on after a culturing experiment, based on which had cellular activity during the experiment. Preliminary results showed that if a cell was left inside a resonator, and periodic measurements were performed, the Q factor began to decrease. This can be attributed to the cell beginning to spread out inside the tube. Further *in situ* measurements with such a sensor could help reveal when a cell is going into mitosis, morphing into a compact ball, or when it is about to undergo apoptosis (due to the cell going into rigor).

4.3 Microfluidic integration of rolled-up optofluidic ring resonators (RU-OFRR)

The microfluidic integration of label-free (bio)sensors is of paramount importance, all the way from analytical science up to the pharmaceutical industry.^{30,107,112–114} A number of standard techniques rely on using off-chip tapered waveguides to couple light into optical cavities, resulting in WGMs which can be used to detect changes in the environment.^{105,113} Standard 2D on-chip waveguides and resonators lack the ability of full optofluidic integration.^{115–117} In an effort to bring all components on-chip, recent results have been reported of coupling light from on-chip waveguides into rolled-up resonators,³⁵ which, as was mentioned earlier, have an advantage to also be used as fluidic channels.¹⁰¹ An integration of a rolled-up optical resonator, being used as a fluidic channel, allows for the sensing of small fluid volumes (that pass through the microtube). This gives rise to a device known as a rolled-up optofluidic ring resonator (RU-OFRR).¹⁰² This integration allows for the ability to detect small changes in the liquid passing through the structure, if the inner wall of the resonator is in contact with the liquid and the outer wall is surrounded by air.¹¹⁸ This means that only sub-picolitre volumes of fluid are required for the label-free detection of the analytes. This integration is very useful since the entire fluidic channel is the sensor, maximizing the cross section of the detector; compared to the cross section a 2D resonator offers, resting at the bottom of a fluidic channel. This in turn, allows for a higher sensitivity: 2D on-chip resonators have been reported to exhibit sensitivities from 70 nm per RIU (refractive index units)¹¹⁵ up to most recently, 246 nm per RIU,¹¹⁷ whereas with 3D RU-OFRR devices, we have achieved sensitivities of 473 nm per RIU and higher.¹⁰²

We have developed a fabrication method to integrate RU-OFRR structures into microfluidic systems.¹⁰² Moreover, it was found that the RU-OFRRs maintain their high optical quality even after being embedded in an SU-8 polymeric structure, Fig. 9(a). The optical resonator (microtube) bridges an inlet and outlet fluidic channel. A viewport, surrounded by air, is positioned in the middle of the RU-OFRR, where the WGMs are measured. Due to the multiple rotations the microtube undergoes during fabrication, the wall of the resonator is relatively thick (about 250 nm thick SiO₂), but still subwavelength. Given the low index of refraction of air, the majority of

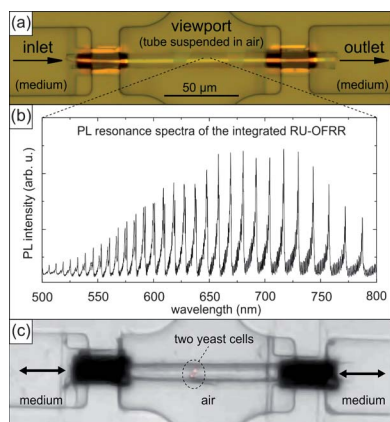


Fig. 9 An integrated RU-OFRR. (a) The inlet and outlet channels as well as the viewport are defined by a polymeric structure (SU-8). The center part of the tube is surrounded by air, a section defined as the “viewport”, and is from where the PL measurements are taken. (b) The depicted PL spectrum is taken from the integrated transparent microtube with no media flowing (air). (c) An image of yeast cells moving through the integrated transparent microtube (see ESI, video S1†).

the light is confined to the higher index wall and the liquid flowing through the structure. The complete chip device consists of the RU-OFRR integrated into the microfluidic structure, sandwiched by a bottom glass substrate and a PDMS top layer with pinholes for connection to a microsyringe pump system. Fig. 9(b) depicts the PL spectrum of an integrated resonator with a quality factor ($Q \approx 10^3$) which is high for being run in an active mode (*i.e.* source of light imbedded in resonator).

Besides the pumping systems mentioned earlier, such as catalytic micropumps or μ -syringe pumping, the use of a classical external pressure controlled system offers another way to precisely manipulate the motion of objects or cells within a tubular structure as shown in Fig. 9(c) (see ESI, Video S1†). In this particular example, two yeast cells are flown back and forth, using a precise pressure control, from the inlet and outlet of the microtube. This is another example that shows the capabilities of rolled-up microtubes being used as optofluidic (bio)sensors. Furthermore, these kinds of devices can be envisioned as new systems for in-flow cytometry.

4.4 Metamaterials

With the discovery of metamaterials, a new class of optics was defined, opening the doors to investigate new optical phenomena previously considered impossible. Metamaterials are man-made materials whose optical properties arise not only from the properties of the individual materials within, but also from the shape/lattice/orientation of the subwavelength structures making up the metamaterial and can be designed to manipulate light.^{32,119–122} A number of recent, particularly exciting, metamaterials are based on plasmonics.¹²³ Plasmonics hinge on a phenomenon in which light couples to oscillating free electrons on the surface of a metal and dielectric, which leads to a propagation of light at shorter-than-free-space wavelengths. Because of these shorter wavelengths, plasmonics can be used to go beyond the diffraction limit of light which is possible, in one instance, with a device known as a hyperlens,^{124–131} discussed below in further detail. These plasmonic metamaterials can be created by multilayer-stacks composed of alternating metal and dielectric.^{129,130} The condition is that each bilayer in the stack is much smaller than the free space wavelength of light traveling through the structure ($d = f_m + f_d \ll \lambda_0$), where d is the overall bilayer thickness and f_m and f_d are the thicknesses of the metal and dielectric, respectively.¹³² When the materials are combined on this length scale, and the structure is comprised of enough layers, the overall architecture can be approximated as a bulk anisotropic material with an effective permittivity, Fig. 10(a). This effective permittivity is broken into two parts, the effective permittivity of the material perpendicular to the stacked layers is given by $\epsilon_{\perp} = \epsilon_r = (\epsilon_m \epsilon_d) / (c_d \epsilon_m + c_m \epsilon_d)$ [radial permittivity for cylindrical structures], and the effective permittivity of the material in-plane to the stacked layers, $\epsilon_{\parallel} = \epsilon_{\theta} = (c_d \epsilon_d + c_m \epsilon_m)$ [tangential permittivity for cylindrical structures].¹³² Here, $c_d + c_m = 1$ are the filling ratio and ϵ_d and ϵ_m are the permittivity of the dielectric and metal, respectively.

Rolled-up nanotech is the perfect approach for creating these multilayer stacked structures, while at the same time reducing the number of processing steps required to make them. By simply rolling up a single bilayer of a metal and oxide (or semiconductor), one can create multilayer stacked metamaterials with a cylindrical geometry.^{29,31,32,52}

By guiding light, at particular wavelengths, radially through a cylindrical metamaterial which is composed of the right bilayer

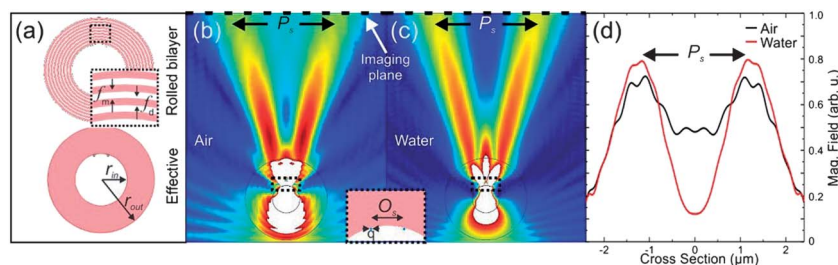


Fig. 10 Rolled-up hyperlens. (a) The permittivity of a rolled-up bilayer structure can be modeled as an anisotropic effective permittivity. Finite element method simulations of a water-impedance matched hyperlens working in (b) air and (c) water. The simulation considered an effective permittivity of a 2 : 1 ratio of Al_2O_3 : Ag at $\lambda_0 = 342$ nm leading to a $\text{sqrt}(\epsilon_{\theta}) = 1.32$ and an index of refraction for water used was 1.33. Inset of (b and c): the geometry used is as follows: an inner diameter $r_{\text{in}} = \lambda_0$, outer diameter $r_{\text{out}} = 3\lambda_0$, a separation of dots $O_s = \lambda_0/2$ and a dot size $q = \lambda_0/30$. (d) The intensity profile taken at the imaging plane shows that the resolution of the quantum dots with a magnification of $\sim 14\times$ is much better for the immersion in water. Adapted from E. J. Smith *et al.* (ref. 31).

combination of materials, the diffraction limit of light can be broken. The evanescent near field emission from an object resting on the inner surface of the tube excites and couples to surface plasmons in the metamaterial. If the metamaterial tube wall is thick enough, this coupling can result in a conversion of the free space evanescent wave into a propagating wave as it exits the structure, which can then propagate in free space and be picked up with classical optics. This is possible if transverse magnetic (TM) waves are being used, which leads to a dispersion relation $k_o^2 = (k_\theta^2/\epsilon_r) + (k_r^2/\epsilon_\theta)$, where k_θ and k_r are the tangential and radial wave vectors respectively. Considering light that is traveling radially out through the structure, k_r is proportional to the wavelength at which the light travels in the metamaterial and k_θ is proportional to the size of the transmitted object. Therefore, if a typical isotropic medium is considered for a lens (*i.e.* $\epsilon_\theta = \epsilon_r$), the isofrequency dispersion relation would be circular, which in turn defines the diffraction limit. If instead, an anisotropic metamaterial (*i.e.* $\epsilon_\theta \neq \epsilon_r$) is used as a lens, the isofrequency dispersion relation can be tuned to either a hyperbola or ellipse, both of which allow for the resolution of subwavelength objects lying on the inner surface of the lens. See ref. 31,125,126,128, and 131 for further details.

The hyperlens has been demonstrated experimentally in the form of a half-cylindrical structure¹²⁹ and significant progress has been made for realizing a rolled-up version of the device.^{29,52} Using a rolled-up hyperlens as a platform, an investigation was carried out to study at what wavelengths it would be possible to achieve hyperlensing.³¹ It was found that by using bilayer combinations of $\text{Al}_2\text{O}_3/\text{Ag}$ and TiO_2/Ag , hyperlensing could be achievable over the entire visible spectrum (an important finding since research depends largely on visible light to observe cellular/biomatter behavior). In addition to this, a method for enhancing the output of the hyperlens was put forth based on impedance matching the tangential component of the effective permittivity of the lens to the surrounding media [$\sqrt{\epsilon_\theta} = n_{\text{medium}}$], a technique known as immersion hyperlensing.³¹ The improved achievable resolution is highlighted in Fig. 10. Fig. 10 shows a hyperlens which is impedance matched to water, operating in air (b), and water (c). A cross section of the intensity, Fig. 10(d), at the imaging plane shows a much better resolution in water (which has a comparable index of refraction to cell culture media¹³³).

The optical microscope is a standard piece of equipment in biology labs; however, despite the greatness of this tool, it is unable to resolve biological details on the size smaller than the observation wavelength. The hyperlens is of very high importance to biological studies as it would allow for the optical *in situ* observation of living organisms, revealing nanometre-sized details that have, until now, remained blurry.

5 Electrical components

Ultracompact electrical components could be extremely beneficial to the lab-in-a-tube system, as it would allow for many *in situ* controlled analyses and manipulation of culture conditions. The expansion into the third dimension^{40,41,134} that rolled-up nanotech offers, enables researchers to decrease the final footprint of devices, which in turn makes it possible to increase the density of on-chip electronic devices. In order to have

working electrical devices, it is important to design and fabricate electrodes which are rolled up with the functional layer, embedding them within the microtube. The demonstration of creating these electrodes was an impressive and important feat for the components of the rolled-up family and have been implemented for developing numerous electrical components including resistors,³⁷ capacitors,^{40,41} superconductors,⁴² magnetic sensors⁵⁵ and heating elements.⁵⁴ This section will give an overview of a number of these rolled-up electrical components which are important to the future of lab-in-a-tube.

5.1 Electrical sensing

One of the first rolled-up components to be characterized electrically³⁸ were rolled-up resistors.³⁷ These resistors were formed using highly B doped SiGe/Si bilayers which were released by selectively etching away an undoped Si sacrificial layer, insets of Fig. 11(a). It was found, that by tuning the active bilayer thickness, the resulting resistance of the microtube could be easily changed from 9 up to 110 k Ω .

Furthermore, rolled-up integrated electrodes inside the microtubular structures can be employed to record currents from neurons or other cells. The application of a voltage from the integrated electrodes may trigger the opening of transmembrane voltage-gated channels such as potassium channels. The motion of the ions through the cellular membrane would then be collected as a current by the second electrode. Substituting typical two electrode voltage-clamp or patch-clamp electrodes by lab-in-a-tube microsystems, with integrated electrodes, might improve the recording efficiency and offer the possibility to record currents at several points located in close vicinity to the specimen. This is of great interest in order to better understand neuronal transmission, especially due to the heterogenic expressions of the different channels involved in action potential generation and transmission.^{135,136}

5.2 Energy storage devices

A number of energy storage devices have been realized through rolled-up nanotech including bulk composites for Li ion batteries,³⁹ off-chip redox-based micro-supercapacitors (using RuO_2 active layers)¹³⁷ and ultracompact integrated on-chip capacitors.⁴⁰ The on-chip electrostatic capacitors are of special interest because they were created with non-toxic compounds. This work introduced a method in which an inorganic sacrificial

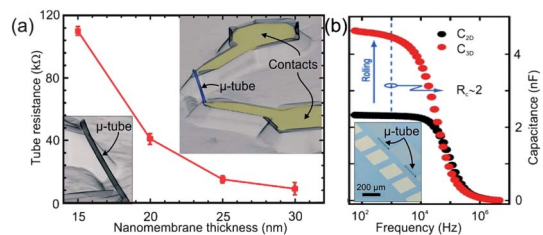


Fig. 11 Rolled-up electronic devices. (a) By tuning the active bilayer ($\text{Si}_{0.5}\text{Ge}_{0.5}\text{B}/\text{SiB}$) thickness of a free-standing microtube, the resistance of the device can be set. Adapted from F. Cavallo *et al.* (ref. 37). (b) Capacitance measurements carried out on rolled-up capacitors are found to have $\sim 2 \times$ higher capacitance to their planar counterparts, all while taking up a smaller footprint. Adapted from C. C. Bof Bufon *et al.* (ref. 40).

layer (Ge) is used, which can be removed in a harmless aqueous solution. The roll-up of the structure creates a mechanical contact between the bottom metal layer and the top oxide layer. This leads to an increase in the final capacitor area. When numerous rotations are performed, this added area allows the device to mimic two planar capacitors connected in parallel. The final capacitance of the 3D structure can be calculated as $C_{3D} = C_{2D}(2 - 1/N)$, where N is the number of windings, $C_{2D} = \kappa_{ox}\epsilon_0 A_{2D}/t_{ox}$ (where t_{ox} and κ_{ox} are the oxide thickness and relative dielectric constant and A_{2D} is the area of the 2D structure that is rolled up).⁴⁰ This equation was confirmed experimentally to reveal a capacitor structure that held a capacitance on the order of $2\times$ that it had in its planar geometry, Fig. 11(b). The work demonstrated a shrink-down of the device footprint of $\sim 25\times$ and a $2\times$ increase of the capacitance, thereby resulting in an increase in the capacitance per footprint from ~ 1.3 to $\sim 200 \mu\text{F cm}^{-2}$.

The relevance of this work to lab-in-a-tube lies in the new method for roll-up in biologically harmless solution, a point not previously established, as well as the energy storage aspect. Since it is of interest to have resistive³⁷ and current measurements in close proximity to the biomatter, taken from built-in sensors, as well as heating elements⁵⁴ for local regulation of the temperature, it would also be important to have an all internal power supply for these components. The rolled-up system would allow for the lab-in-a-tube device to be directly connected to a nearby rolled-up capacitor or battery, supplying it with the necessary power.

5.3 Heating elements

Microfluidic devices are particularly well-suited to be developed with rolled-up nanotech due to the possibility of creating active devices by means of electrical and thermal functionalization of the tubes, in combination with special organic filling materials. Temperature-sensitive hydrogels are able to change their swelling state if a lower critical solution temperature (LCST) is exceeded.¹³⁸ This effect can be used to realize valve-like devices for microfluidics.¹³⁹

An important step towards realization of this concept, by fabrication of compact rolled-up heater devices, for fluidic applications using rolled-up nanotech, was recently reported.⁵⁴ The heating elements on the surface of these devices should provide a temperature above the LCST value. Therefore, for the application of this work, three key layers are needed: (i) a heating layer, (ii) a temperature sensing layer and (iii) a thermal, highly conducting layer for fast thermal transport, in order to obtain a fast temporal response of the devices. In the device architecture, an additional material was introduced for strain generation, which, at the same time, acts as a thermal conductor in the working regime of the device.

Infrared measurements were carried out as follows: the heater voltage was increased at a rate of 0.05 V s^{-1} from zero up to 12 V. The planar heater generates an extended temperature field with a large diameter, Fig. 12(a), whereas the rolled-up device produces heat almost exclusively within the volume taken up by the rolled-up layer stack, Fig. 12(b), providing extremely localized heating. The behavior of the planar heater can be explained by the high isotropic thermal conductivity of the

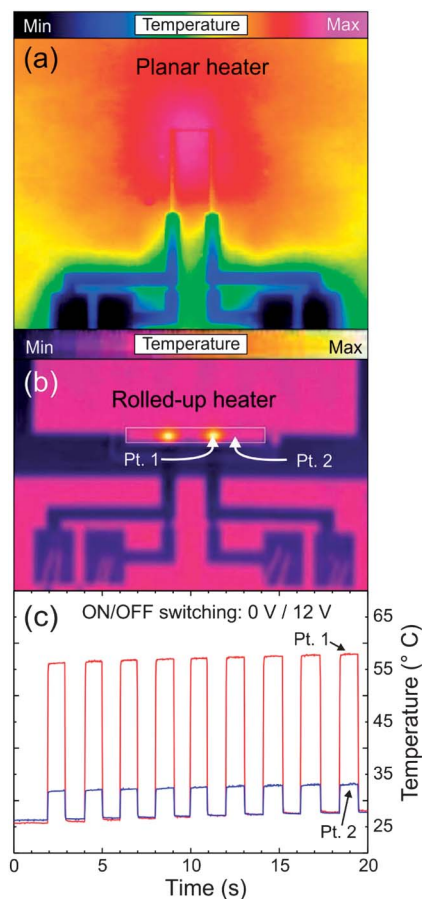


Fig. 12 Rolled-up heating elements. Thermo-camera images from a heater device in (a) planar and (b) rolled-up configuration. (c) Dynamic behavior of a rolled-up heater with a diameter of $\sim 60 \mu\text{m}$ for a ON (12 V:0.01 A)/OFF (0 V) cycling of the heater voltage. Adapted from I. Mönch *et al.* (ref. 54).

silicon wafer used as a substrate and being in intimate contact with the deposited layers. In contrast, the rolled-up structure has only a line-shaped contact with the substrate, thus suppressing the thermal conductivity to the substrate.

By switching the current ON and OFF, the reaction of the heater element to periodic changes in the power supply was investigated. In the temperature vs. time diagram recorded at the center of the rolled-up heater, it was observed that the temperature follows the heating power at a very fast rate, on the order of 0.04 s, Fig. 12(c). The reason for this excellent dynamic characteristic can be explained by the thermal decoupling of the tube-like heater from the substrate and by the high thermal conductivity of the auxiliary CuNiMn rolled-up film. This system is also well-suited for a localized incubation study on individual cellular and bacterial growths.

5.4 Magnetic sensors

Recently, rolled-up nanotech was employed to fabricate compact cylindrical magnetic sensor devices,⁵⁵ which can be straightforwardly integrated into existing fluidic architectures, Fig. 13(a). Functional nanomembranes, consisting of a magnetic sensor element based on 30 multilayers of [Py/Cu] revealing GMR, were

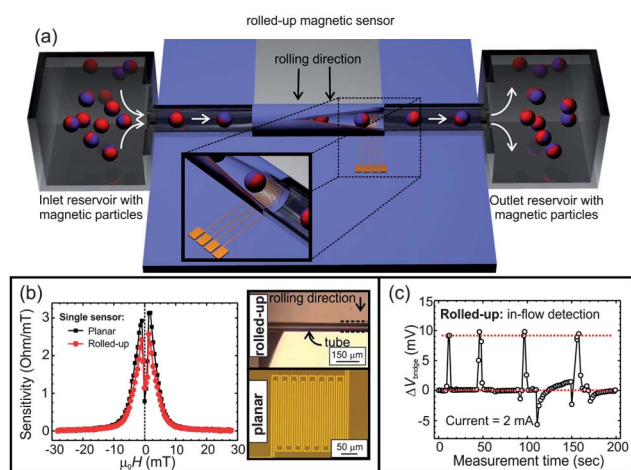


Fig. 13 Rolled-up magnetic sensors.⁵⁵ (a) A schematic highlighting the principle of the in-flow detection of individual CrO_2 nanoparticles through a rolled-up magnetic sensor. (b) A comparison of the sensitivity of the planar and rolled-up magnetic sensors. Insets are two photographs of the meander-like GMR sensor before (bottom) and after (top) the roll-up process. (c) The signal readout from the sensor as individual magnetic particle passes through the tube. Adapted from I. Mönch *et al.* (ref. 55).

rolled up. The sensor's characteristics before and after the roll-up process were found to be similar, Fig. 13(b), allowing for a reliable and predictable method to fabricate high quality ultracompact GMR devices. The performance of the rolled-up magnetic sensor was optimized to achieve high sensitivity to weak magnetic fields, as required in biomedical applications (in the range of 0.1 mT): (i) the GMR multilayers were coupled in the second antiferromagnetic maximum, providing high sensitivity to low magnetic fields and (ii) the sensors were arranged in a Wheatstone bridge configuration, leading to an improved differential sensitivity and thermal stability.

As was also demonstrated earlier, the rolled-up tube itself can be efficiently used as a fluidic channel, while the integrated magnetic sensor provides an important functionality to detect and respond to a magnetic field. The performance of the rolled-up magnetic sensor for the in-flow detection of ferromagnetic CrO_2 nanoparticles embedded in a biocompatible polymeric hydrogel shell was highlighted, Fig. 13(c). This sensing concept could easily be extended to detect magnetically functionalized organisms or magnetotactic bacteria.^{140,141} The advantages of this device are intriguing: (i) the sensor covers part of the inner wall of the fluidic channel, and as such, is positioned in the closest possible vicinity to the flowing objects. This increases the signal to noise ratio of the device compared to the case when the sensor is positioned outside of the channel. (ii) The rolled-up geometry makes the sensor sensitive to magnetic stray fields of the particles under study in virtually all directions. This avoids implementation of an external magnet to align the magnetic moment of the particle relative to the position of the sensor. Both these aspects are crucial for efficient and successful in-flow detection of magnetic objects.

This approach could be beneficial for efficient biodetection of protein structures,¹⁴² diagnostics of diseases,¹⁴³ counting and sorting of living cells with internalized magnetic nanoparticles,^{144,145} or functionalized nanocontainers.^{146,147} The advantage

of rolled-up magnetic devices^{55,148–152} is their straightforward integrability into existing on-chip technologies and the ability to combine several functions into a single architecture, possibly leading to a fully operational lab-in-a-tube system.

6 Conclusions

In summary, we have reviewed the recent advances in ultracompact, rolled-up components which can be, and are planned to become, an integral part of lab-in-a-tube total analysis systems. An overview of what lab-in-a-tube is and what advantages it brings to the biosensing and exploration of organisms was highlighted in a number of ways. These advantages include arrays of 3D microtubular scaffolding which can be functionalized to mimic the ECM for the culture and investigation of individual organisms. Each microtube would have a number of components integrated within to make important electrical, magnetic and optical *in situ* observations.

Various off-chip and on-chip methods for the capture of biomaterial within the confinements of the microtubes were presented. These comprised microsyringe, micropump, optical trap, and chemical pumping systems. Numerous cellular culture studies have been performed over the past years in conjunction with the 3D scaffolding structures. These have included (i) the study of microtube size dependence on the proliferation of yeast cells; (ii) the micro organization, based on tubular arrays, provided for neuron cell networks; (iii) as well as detailed study of HeLa cell proliferation at various stages of growth within functionalized microtubes.

On the detection side, a review of the optical, electrical and magnetic components, which have been investigated and can be incorporated into lab-in-a-tube, was given. Optical sensors based on optical ring resonators were shown to be capable of detecting differences in the surrounding media through shifts in WGM peaks and the optomechanical detection of oversized fibroblasts was demonstrated with F-SW μ RS. Metamaterials also show promise in the near future for the ability to manipulate light and reveal subwavelength details about the objects of interest with devices such as the hyperlens. With the integration of electrodes into rolled-up structures it was possible to create a number of electrical devices. Resistive changes of organisms could potentially be monitored with built-in resistors. Heating devices could be used for either creating valves in microfluidic systems or studying proximity incubation effects in single cell growth. Magnetic sensors were introduced which demonstrated the ability to detect stray magnetic fields from microobjects passing through the rolled-up architectures. Given that all of these electrical devices would need some form of power supply, a look at cutting edge, rolled-up capacitors was given as well. It is important to point out that, although electrochemical methods are not presented in this work, extensive work towards the use of electrodes for manipulation, stimulation and detection of molecules and organisms is currently being explored using the lab-in-a-tube platform.

Lab-in-a-tube offers a great opportunity in both reducing the size of lab-on-a-chip systems as well as allowing for a large number of data points taken from individual organisms under similar growth conditions. The next step which needs to be taken in this exploration is to further construct rolled-up systems which

combine a number of the individual ultracompact components mentioned here into single devices, like the RU-OFRR system presented earlier. At the same time it is also of interest to continue pushing the edge of what types of components can be created for such a system including new electronics and safe pumping systems. It is expected in the near future that these steps will be made, allowing for the possibility of lab-in-a-tube systems to bring an important role in helping with diagnostics and to further our understanding of the biological systems around us.

Acknowledgements

This work was funded by the Volkswagen Foundation (I/84 072), by a Multidisciplinary University Research Initiative (MURI) sponsored by the U. S. Air Force Office of Scientific Research (AFOSR) (FA9550-09-0550) as well as by German Science Foundation (DFG) grants MO887/1-2, AR193/11-2 and DFG Research Unit 1713 "Sensoric Micro- and Nanosystems."

References

- 1 A. Manz, N. Graber and H. M. Widmer, *Sens. Actuators, B*, 1990, **1**, 244.
- 2 G. M. Whitesides, *Nature*, 2005, **442**, 368.
- 3 M. Khine, A. Lau, C. Ionescu-Zanetti, J. Seo and L. P. Lee, *Lab Chip*, 2005, **5**, 38.
- 4 D. Di Carlo, C. Ionescu-Zanetti, Y. Zhang, P. Huang and L. P. Lee, *Lab Chip*, 2005, **5**, 171.
- 5 A. Tourovskaia, X. Figueroa-Masot and A. Folch, *Lab Chip*, 2005, **5**, 14.
- 6 J. El-Ali, P. K. Sorger and K. F. Jensen, *Nature*, 2006, **442**, 403.
- 7 A. G. Crevillén, M. Pumera, M. C. González and A. Escarpa, *Lab Chip*, 2009, **9**, 346.
- 8 M. Pumera, *Chem. Commun.*, 2011, **47**, 5671.
- 9 A. J. deMello, *Nature*, 2006, **442**, 394.
- 10 A. G. Crevillén, A. Ávila, M. Pumera, M. C. González and A. Escarpa, *Anal. Chem.*, 2007, **79**, 7408.
- 11 A. G. Crevillén, M. Pumera, M. C. González and A. Escarpa, *Electrophoresis*, 2008, **29**, 2997.
- 12 M. Pumera, *Electrophoresis*, 2008, **29**, 269.
- 13 X. Llopis, M. Pumera, S. Alegret and A. Merkoçi, *Lab Chip*, 2009, **9**, 213.
- 14 F. Lefèvre, A. Chalifour, L. Yu, V. Chodavarapu, P. Juneau and R. Izquierdo, *Lab Chip*, 2012, **12**, 787.
- 15 M. I. Stockman, *Phys. Today*, 2011, February, 39.
- 16 T. Endo, K. Kerman, N. Nagatani, H. M. Hiepa, D. K. Kim, Y. Yonezawa, K. Nakano and E. Tamiza, *Anal. Chem.*, 2006, **78**, 6465.
- 17 G. G. Stoney, *Proc. R. Soc. London, Ser. A*, 1909, **82**, 172.
- 18 O. G. Schmidt, N. Schmarje, C. Deneke, C. Müller and N. Y. Jin-Phillipp, *Adv. Mater.*, 2001, **13**, 756.
- 19 V. Y. Prinz, V. A. Seleznev, A. K. Gutakovskiy, A. V. Chehovskiy, V. V. Preobrazenskii, M. A. Putyato and T. A. Gavrilova, *Phys. E.*, 2000, **6**, 828.
- 20 O. G. Schmidt and K. Eberl, *Nature*, 2001, **410**, 168.
- 21 Y. F. Mei, G. S. Huang, A. A. Solovev, E. Bermúdez Ureña, I. Mönch, F. Ding, T. Reindl, R. K. Y. Fu, P. K. Chu and O. G. Schmidt, *Adv. Mater.*, 2008, **20**, 4085.
- 22 M. Huang, F. Cavallo, F. Liu and M. G. Lagally, *Nanoscale*, 2011, **3**, 96.
- 23 E. J. Smith, D. Makarov and O. G. Schmidt, *Soft Matter*, 2011, **7**, 11309.
- 24 J. A. Rogers, M. G. Lagally and R. G. Nuzzo, *Nature*, 2011, **447**, 45.
- 25 T. Kipp, H. Welsch, C. Strelow, C. Heyn and D. Heitmann, *Phys. Rev. Lett.*, 2006, **96**, 077403.
- 26 S. Mendach, R. Songmuang, S. Kiravittaya, M. Benoucef and O. G. Schmidt, *Appl. Phys. Lett.*, 2006, **88**, 111120.
- 27 R. Songmuang, A. Rastelli, S. Mendach, C. Deneke and O. G. Schmidt, *Microelectron. Eng.*, 2007, **84**, 1427.
- 28 E. J. Smith, S. Schulze, S. Kiravittaya, Y. F. Mei, S. Sanchez and O. G. Schmidt, *Nano Lett.*, 2011, **11**, 4037.
- 29 S. Schwaiger, M. Bröll, A. Krohn, A. Stemmann, C. Heyn, Y. Stark, D. Stickler, D. Heitmann and S. Mendach, *Phys. Rev. Lett.*, 2009, **102**, 163903.
- 30 G. S. Huang, V. A. Bolaños Quiñones, F. Ding, S. Kiravittaya, Y. F. Mei and O. G. Schmidt, *ACS Nano*, 2010, **4**, 3123.
- 31 E. J. Smith, Z. Liu, Y. F. Mei and O. G. Schmidt, *Appl. Phys. Lett.*, 2009, **95**, 083104; E. J. Smith, Z. Liu, Y. F. Mei and O. G. Schmidt, *Appl. Phys. Lett.*, 2010, **96**, 019903.
- 32 E. J. Smith, Z. Liu, Y. F. Mei and O. G. Schmidt, *Nano Lett.*, 2010, **10**, 1.
- 33 F. Li and Z. Mi, *Opt. Express*, 2009, **17**, 19933.
- 34 S. Vicknesh, F. Li and Z. Mi, *Appl. Phys. Lett.*, 2009, **94**, 081101.
- 35 Z. Tian, V. Veerasubramanian, P. Bianucci, S. Mukherjee, Z. Mi, A. G. Kirk and D. V. Plant, *Opt. Express*, 2011, **19**, 12164.
- 36 A. A. Solovev, S. Sanchez, Y. F. Mei and O. G. Schmidt, *Phys. Chem. Chem. Phys.*, 2011, **13**, 10131.
- 37 F. Cavallo, R. Songmuang and O. G. Schmidt, *Appl. Phys. Lett.*, 2008, **93**, 143113.
- 38 S. V. Golod, V. Y. Prinz, V. I. Mashanov and A. K. Gutakovskiy, *Semicond. Sci. Technol.*, 2001, **16**, 181.
- 39 H. X. Ji, X. L. Wu, L. Z. Fan, C. Krien, I. Fiering, Y. G. Guo, Y. F. Mei and O. G. Schmidt, *Adv. Mater.*, 2010, **22**, 4591.
- 40 C. C. Bof Bufon, J. D. Cojal González, D. J. Thurmer, D. Grimm, M. Bauer and O. G. Schmidt, *Nano Lett.*, 2010, **10**, 2506.
- 41 C. C. Bof Bufon, J. D. Arias Espinoza, D. J. Thurmer, M. Bauer, C. Deneke, U. Zschieschang, H. Klauk and O. G. Schmidt, *Nano Lett.*, 2011, **11**, 3727.
- 42 D. J. Thurmer, C. C. Bof Bufon, C. Deneke and O. G. Schmidt, *Nano Lett.*, 2010, **10**, 3704.
- 43 G. S. Huang, Y. F. Mei, D. J. Thurmer, E. Coric and O. G. Schmidt, *Lab Chip*, 2009, **9**, 263.
- 44 S. Schulze, G. S. Huang, M. Krause, D. Aubyn, V. A. Bolaños Quiñones, C. K. Schmidt, Y. F. Mei and O. G. Schmidt, *Adv. Eng. Mater.*, 2010, **12**, B558.
- 45 M. Yu, Y. Huang, J. Ballweg, H. Shin, M. Huang, D. E. Savage, M. G. Lagally, E. W. Dent, R. H. Blick and J. C. Williams, *ACS Nano*, 2011, **5**, 2447.
- 46 S. Zakharchenko, E. Sperling and L. Ionov, *Biomacromolecules*, 2011, **12**, 2211.
- 47 W. Xi, C. K. Schmidt, D. H. Gracias, E. J. Smith, S. Sanchez and O. G. Schmidt, unpublished.
- 48 Y. F. Mei and O. G. Schmidt, 2008, Volkswagen project proposal, Grant No. I/8072.
- 49 E. J. Smith, Y. F. Mei and O. G. Schmidt, *Proc. SPIE*, 2011, **8031**, 80310R, DOI: 10.1117/12.885246.
- 50 G. S. Huang, S. Kiravittaya, V. A. Bolaños Quiñones, F. Ding, M. Benoucef, A. Rastelli, Y. F. Mei and O. G. Schmidt, *Appl. Phys. Lett.*, 2009, **94**, 141901.
- 51 F. Li, S. Vicknesh and Z. Mi, *Electron. Lett.*, 2009, **45**, 645.
- 52 S. Schwaiger, M. Klingbeil, J. Kerbst, A. Rottler, R. Costa, A. Koitmäe, M. Bröll, C. Heyn, Y. Stark, D. Heitmann and S. Mendach, *Phys. Rev. B: Condens. Matter Mater. Phys.*, 2011, **84**, 155325.
- 53 S. Sanchez, A. A. Solovev, Y. F. Mei and O. G. Schmidt, *J. Am. Chem. Soc.*, 2010, **132**, 13144.
- 54 I. Mönch, J. Schumann, M. Stockmann, K. F. Arndt and O. G. Schmidt, *Smart Mater. Struct.*, 2011, **20**, 085016.
- 55 I. Mönch, D. Makarov, R. Koseva, L. Baraban, D. Karnauschenko, C. Kaiser, K. F. Arndt and O. G. Schmidt, *ACS Nano*, 2011, **5**, 7436.
- 56 *Chromatography and Capillary Electrophoresis in Food Analysis*, ed. H. Sørensen, S. Sørensen, C. Bjerregaard and S. Michaelsen, The Royal Society of Chemistry, Cambridge, 1999, p. 181.
- 57 W. F. Paxton, P. T. Baker, T. R. Kline, Y. Wang, T. E. Mallouk and A. Sen, *J. Am. Chem. Soc.*, 2006, **128**, 14881.
- 58 Y. Hong, M. Diaz, U. M. Córdova-Figueroa and A. Sen, *Adv. Funct. Mater.*, 2010, **20**, 1568.
- 59 A. Ashkin, *Phys. Rev. Lett.*, 1970, **24**, 156.
- 60 P. Y. Chiou, A. T. Ohta and M. C. Wu, *Nature*, 2005, **436**, 370.
- 61 M. J. Lang, P. M. Fordyce, A. M. Engh, K. C. Neuman and S. M. Block, *Nat. Methods*, 2004, **1**, 133.
- 62 K. C. Neuman and A. Nagy, *Nat. Methods*, 2008, **5**, 491.
- 63 H. Zhang and K. K. Liu, *J. R. Soc. Interface*, 2008, **5**, 671.
- 64 E. M. Purcell, *Am. J. Phys.*, 1977, **45**, 3.

- 65 T. R. Kline, W. F. Paxton, Y. Wang, D. Velegol, T. E. Mallouk and A. Sen, *J. Am. Chem. Soc.*, 2005, **127**, 17150; T. R. Kline, J. Iwata, P. E. Lammert, E. E. Mallouk, A. Sen and D. Velegol, *J. Phys. Chem. B*, 2006, **110**, 24513; S. Subramanian and J. M. Catchmark, *J. Phys. Chem. C*, 2007, **111**, 11959; M. E. Ibele, Y. Wang, T. R. Kline, T. E. Mallouk and A. Sen, *J. Am. Chem. Soc.*, 2007, **129**, 7762.
- 66 Y. H. Choi, S. U. Son and S. S. Lee, *Sens. Actuators, A*, 2004, **111**, 8; A. Takashima, K. Kojima and H. Suzuki, *Anal. Chem.*, 2010, **82**, 6870.
- 67 A. A. Solovov, E. J. Smith, C. C. Bof Bufon, S. Sanchez and O. G. Schmidt, *Angew. Chem., Int. Ed.*, 2011, **50**, 10875; A. A. Solovov, E. J. Smith, C. C. Bof Bufon, S. Sanchez and O. G. Schmidt, *Angew. Chem.*, 2011, **123**, 11067.
- 68 S. Sanchez, A. N. Ananth, V. M. Fomin, M. Viehrig and O. G. Schmidt, *J. Am. Chem. Soc.*, 2011, **36**, 3840.
- 69 M. Ibele, T. E. Mallouk and A. Sen, *Angew. Chem., Int. Ed.*, 2009, **48**, 3308.
- 70 A. S. Andersson, P. Olsson, U. Lidberg and D. Sutherland, *Exp. Cell Res.*, 2003, **288**, 177.
- 71 E. A. Cox, S. K. Sastry and A. Huttenlocher, *Mol. Biol. Cell*, 2001, **12**, 265.
- 72 M. J. Dalby, M. O. Riehle, H. Johnstone, S. Affrossman and A. S. G. Curtis, *Biomaterials*, 2002, **23**, 2945.
- 73 D. E. Ingber, *Proc. Natl. Acad. Sci. U. S. A.*, 2003, **100**, 1472.
- 74 M. S. Molly and H. G. Julian, *Science*, 2005, **310**, 1135.
- 75 S. F. Badylak, *Transplant Immunol.*, 2004, **12**, 367.
- 76 S. F. Badylak, *Biomaterials*, 2007, **28**, 3587.
- 77 I. Patla, T. Volberg, N. Elad, V. Hirschfeld-Warneken, C. Grashoff, R. Fässler, J. P. Spatz, B. Geiger and O. Medalia, *Nat. Cell Biol.*, 2010, **12**, 909.
- 78 J. A. Deeg, L. Louban, D. Avdin, C. Selhuber-Unkel, H. Kessler and J. P. Spatz, *Nano Lett.*, 2011, **11**, 1469.
- 79 P. J. Hung, P. J. Philip, P. Sabouchi, R. Lin and L. P. Lee, *Biotechnol. Bioeng.*, 2005, **89**, 1.
- 80 V. M. Weaver, O. W. Petersen, F. Wang, C. A. Larabell, P. Briand, C. Damsky and M. J. Bissell, *J. Cell Biol.*, 1997, **137**, 231.
- 81 S. R. Peyton, C. B. Raub, V. P. Keschrumer and A. J. Putnam, *Biomaterials*, 2006, **27**, 4881.
- 82 T. W. Ridky, J. M. Chow, D. J. Wong and P. A. Khavari, *Nat. Med.*, 2010, **16**, 1450.
- 83 E. Millerot-Serruot, M. Guilbert, N. Fourre, W. Witkowski, G. Saïd, L. V. Gulick, C. Terryn, J. M. Zahm, R. Garnotel and P. Jeannesson, *Cancer Cell Int.*, 2010, **10**, 26.
- 84 D. A. Bruyewicz, A. P. McGuigan and G. M. Whitesides, *Lab Chip*, 2008, **8**, 663.
- 85 T. Sun, D. Norton, J. W. Mckean, A. J. Ryan and S. MacNeil, *Biotechnol. Bioeng.*, 2007, **97**, 1318.
- 86 Y. B. Zhu, K. S. Chian, M. B. Chan-Park, P. S. Mhaisalkar and B. D. Ratner, *Biomaterials*, 2006, **27**, 68.
- 87 C. L. Randall, Y. V. Kalinin, M. Jamal, T. Manohar and D. H. Gracias, *Lab Chip*, 2011, **11**, 127.
- 88 A. Azam, K. Laffin, M. Jamal, R. Fernandes and D. H. Gracias, *Biomed. Microdevices*, 2010, **13**, 51.
- 89 S. H. Lee, H. E. Jeong, M. C. Park, J. Y. Hur, H. S. Cho, S. H. Park and K. Y. Suh, *Adv. Mater.*, 2008, **20**, 788.
- 90 S. M. Harazim, W. Xi, C. K. Schmidt, S. Sanchez and O. G. Schmidt, *J. Mater. Chem.*, 2012, **22**, 2878.
- 91 A. Compston, J. Zajicek, J. Sussman, A. Webb, G. Hall and D. Muir, *J. Anat.*, 1997, **190**, 161.
- 92 D. L. Sherman and P. J. Brophy, *Nat. Rev. Neurosci.*, 2005, **6**, 683.
- 93 D. M. Ackermann, N. Bhadra, E. L. Foldes, X. Wang and K. L. Kilgore, *IEEE Trans. Neural Syst. Rehabil. Eng.*, 2010, **18**, 658.
- 94 M. A. Schiefer, K. H. Polasek, R. J. Triolo, G. C. Pinault and D. J. Tyler, *J. Neural Eng.*, 2010, **7**, 026006.
- 95 X. Navarro, T. B. Krueger, N. Lago, S. Micera, T. Stieglitz and P. A. Dario, *J. Peripher. Nerv. Syst.*, 2005, **10**, 229.
- 96 P. Steigemann, C. Wurzenberger, M. H. Schmitz, M. Held, J. Guizzetti, S. Maar and D. W. Gerlich, *Cell*, 2009, **136**, 473.
- 97 M. Thery, A. Jimenez-Dalmaroni, V. Racine, M. Bornens and F. Julicher, *Nature*, 2007, **447**, 493.
- 98 M. Thery, V. Racine, A. Pepin, M. Piel, Y. Chen, J. B. Sibarita and M. Bornens, *Nat. Cell Biol.*, 2005, **7**, 947.
- 99 A. Pitaval, Q. Z. Tseng, M. Bornens and M. Thery, *J. Cell Biol.*, 2010, **191**, 303.
- 100 N. Minc, S. V. Bratman, R. Basu and F. Chang, *Curr. Biol.*, 2009, **19**, 83.
- 101 D. J. Thurmer, Ch. Deneke, Y. F. Mei and O. G. Schmidt, *Appl. Phys. Lett.*, 2006, **89**, 223507.
- 102 S. Harazim, V. A. Bolaños Quiñones, S. Kiravittaya, S. Sanchez and O. G. Schmidt, unpublished.
- 103 V. A. Bolaños Quiñones, G. S. Huang, J. D. Plumhof, S. Kiravittaya, A. Rastelli, Y. F. Mei and O. G. Schmidt, *Opt. Lett.*, 2009, **34**, 2345.
- 104 K. Dietrich, C. Strelow, C. Schliehe, C. Heyn, A. Stemmann, S. Schaiger, S. Mendach, A. Mews, H. Weller, D. Heitmann and T. Kipp, *Nano Lett.*, 2010, **10**, 627.
- 105 F. Vollmer and S. Arnold, *Nat. Methods*, 2008, **5**, 591.
- 106 H. Zhu, I. M. White, J. D. Suter, P. S. Dale and X. Fan, *Opt. Express*, 2007, **15**, 9139.
- 107 F. Vollmer, S. Arnold and D. Keng, *Proc. Natl. Acad. Sci. U. S. A.*, 2008, **105**, 20701.
- 108 M. Hosoda and T. Shigaki, *Appl. Phys. Lett.*, 2007, **90**, 181107.
- 109 J. Zhu, S. Kaya Ozdemir, Y. F. Xiao, L. Li, L. He, D. R. Chen and L. Yang, *Nat. Photonics*, 2010, **4**, 46.
- 110 T. J. Kippenberg, *Nat. Photonics*, 2010, **4**, 9.
- 111 A. Mazzei, S. Göttinger, L. de S. Menezes, G. Zumofen, O. Benson and V. Sandoghdar, *Phys. Rev. Lett.*, 2007, **99**, 173603.
- 112 J. Hong, J. B. Edel and A. J. deMello, *Drug Discovery Today*, 2009, **14**, 134.
- 113 K. Scholten, X. Fan and E. T. Zellers, *Appl. Phys. Lett.*, 2011, **99**, 141108.
- 114 X. Zhang, L. Ren, X. Wu, H. Li, L. Liu and L. Xu, *Opt. Express*, 2011, **19**, 22242.
- 115 K. De Vos, I. Bartolozzi, E. Schacht, P. Bienstman and R. Baets, *Opt. Express*, 2007, **15**, 7610.
- 116 A. Ramachandran, S. Wang, J. Clarke, S. J. Ja, D. Goad, L. Wald, E. M. Flood, E. Knobbe, J. V. Hryniewicz, S. T. Chu, D. Gill, W. Chen, O. King and B. E. Little, *Biosens. Bioelectron.*, 2008, **23**, 939.
- 117 C. F. Carlborg, K. B. Gylfason, A. Kazmiercyk, F. Dortu, M. J. Bañuls Polo, A. Maquieira Catala, G. M. Kresbach, H. Sohlström, T. Moh, L. Vivien, J. Popplewell, G. Ronan, C. A. Barrios, G. Stemme and W. van der Wijngaart, *Lab Chip*, 2010, **10**, 281.
- 118 A. Bernardi, S. Kiravittaya, A. Rastelli, R. Songmuang, D. J. Thurmer, M. Benyoucef and O. G. Schmidt, *Appl. Phys. Lett.*, 2008, **93**, 094106.
- 119 V. G. Veselago, *Sov. Phys. Usp.*, 1968, **10**, 509.
- 120 J. B. Pendry, *Phys. Rev. Lett.*, 2000, **85**, 3966.
- 121 R. A. Shelby, D. R. Smith and S. Schultz, *Science*, 2001, **292**, 77.
- 122 W. Cai, U. K. Chettiar, A. V. Kildishev and V. M. Shalaev, *Nat. Photonics*, 2007, **1**, 224.
- 123 W. L. Barnes, A. Dereux and T. W. Ebbesen, *Nature*, 2003, **292**, 77.
- 124 B. Wood and J. B. Pendry, *Phys. Rev. B: Condens. Matter Mater. Phys.*, 2006, **74**, 115116.
- 125 A. Salandrino and N. Engheta, *Phys. Rev. B: Condens. Matter Mater. Phys.*, 2006, **74**, 075103.
- 126 Z. Jacob, L. V. Alekseyev and E. E. Narimanov, *Opt. Express*, 2006, **14**, 8247.
- 127 A. V. Kildishev and E. E. Narimanov, *Opt. Lett.*, 2007, **32**, 3432.
- 128 H. Lee, Z. Liu, Y. Xiong, C. Sun and X. Zhang, *Opt. Express*, 2007, **15**, 15886.
- 129 Z. Liu, H. Lee, Y. Xiong, C. Sun and X. Zhang, *Science*, 2007, **315**, 1686.
- 130 J. Rho, Z. Ye, Y. Xiong, X. Yin, Z. Liu, H. Choi, G. Bartal and X. Zhang, *Nat. Commun.*, 2010, **1**, 143.
- 131 C. B. Ma, R. Aguinaldo and Z. Liu, *Chin. Sci. Bull.*, 2010, **55**, 2618.
- 132 S. M. Rytov, *Soviet Physics - JETP*, 1955, **29**, 605.
- 133 D. Borja, F. Manns, A. Ho, N. Ziebarth, A. M. Rosen, R. Jain, A. Amelinckx, E. Arrieta, R. C. Augusteyn and J. M. Parel, *Invest. Ophthalmol. Visual Sci.*, 2008, **49**, 2541.
- 134 D. H. Gracias, J. Tien, T. L. Breen, C. Hsu and G. M. Whitesides, *Science*, 2000, **289**, 1170.
- 135 M. N. Rasband, *Neurosci. Lett.*, 2010, **486**, 101.
- 136 C. Gu and J. Barry, *Prog. Neurobiol.*, 2011, **94**, 115.
- 137 H. X. Ji, Y. F. Mei and O. G. Schmidt, *Chem. Commun.*, 2010, **46**, 3881.
- 138 E. D. Klug, *J. Polym. Sci.*, 1971, **C36**, 491.
- 139 K. F. Arndt, A. Richter, I. Mönch, in Synthesis of stimuli-sensitive hydrogels in the micrometer and sub-micrometer range by radiation techniques and their applications, *Hydrogels, Biological Properties*

- and Applications, ed. R. Barbucci, Springer Science and Business Media, Italia, Milan, 2009, p. 21.
- 140 R. Blakemore, *Science*, 1975, **190**, 377.
- 141 R. B. Frankel, R. P. Blakemore and R. S. Wolfe, *Science*, 1978, **203**, 1355.
- 142 J. M. Nam, C. C. Thaxton and C. A. Mirkin, *Science*, 2003, **301**, 1884.
- 143 J. Baudry, C. Rouzeau, C. Goubault, C. Robic, L. Cohen-Tannoudji, A. Koenig, E. Bertrand and J. Bibette, *Proc. Natl. Acad. Sci. U. S. A.*, 2006, **103**, 16076.
- 144 I. Mönch, A. Meye, A. Leonhardt, K. Kramer, R. Kozhuhrova, T. Gemming, M. P. Wirth and B. Büchner, *J. Magn. Magn. Mater.*, 2005, **290–291**, 276.
- 145 M. Chabert and J. L. Viovy, *Proc. Natl. Acad. Sci. U. S. A.*, 2008, **105**, 3191.
- 146 I. Mönch, A. Meye and A. Leonhardt, *Nanotechnologies for the Life Sciences*, ed. C. S. S. R. Kumar, Wiley-VCH, 2006, **6**, 259.
- 147 I. Mönch, A. Leonhardt, A. Meye, S. Hampel, R. Kozhuharova-Koseva, D. Elefant, M. P. Wirth and B. Büchner, *J. Phys. Conf. Ser.*, 2007, **61**, 820.
- 148 S. Mendach, J. Podbielski, J. Topp, W. Hansen and D. Heitmann, *Appl. Phys. Lett.*, 2008, **93**, 262501.
- 149 F. Ballhorn, S. Mansfeld, A. Krohn, J. Topp, W. Hansen, D. Heitmann and S. Mendach, *Phys. Rev. Lett.*, 2010, **104**, 037205.
- 150 C. Müller, G. B. de Souza, A. Mikowski, O. G. Schmidt, C. M. Lepienski and D. G. Mosca, *J. Appl. Phys.*, 2011, **110**, 044326; C. Müller, M. S. Khatri, C. Deneke, S. Fähler, Y. F. Mei, E. Bermúdez Ureña and O. G. Schmidt, *Appl. Phys. Lett.*, 2009, **94**, 102510.
- 151 E. Bermúdez Ureña, Y. F. Mei, E. Coric, D. Makarov, M. Albrecht and O. G. Schmidt, *J. Phys. D: Appl. Phys.*, 2009, **42**, 055001.
- 152 E. J. Smith, D. Makarov, S. Sanchez, V. M. Fomin and O. G. Schmidt, *Phys. Rev. Lett.*, 2011, **107**, 097204.